Carbon atom adsorption on and diffusion into Fe(110) and Fe(100) from first principles

D. E. Jiang and Emily A. Carter
Department of Chemistry & Biochemistry, Box 951569, University of California, Los Angeles, California 90095-1569, USA
(Received 23 July 2004; published 6 January 2005)

We employ spin-polarized periodic density functional theory (DFT) to examine carbon atom adsorption on, absorption in, and diffusion into Fe(110) and Fe(100). We find that carbon atoms bind strongly with Fe surfaces and prefer high coordination sites. The carbon atom is predicted to adsorb on the long-bridge site on Fe(110) and the fourfold hollow site on Fe(100). Due to the very short distance between the carbon atom and the subsurface Fe atom of Fe(100), the carbon atom binds more strongly with Fe(100) than with Fe(110). In the subsurface region, the carbon atom prefers the octahedral site, as in bulk Fe. We find that the carbon atom is more stable in the subsurface octahedral site of Fe(110) than that of Fe(100), since the strain caused by the interstitial carbon atom is released by pushing one surface Fe atom towards vacuum by 0.5 Å in Fe(110), while the distortion in Fe(100) propagates far into the lattice. Diffusion of carbon atoms into Fe(110) and Fe(100) subsurfaces goes through transition states where the carbon atom is coordinated to four Fe atoms. The barriers to diffusion into Fe(110) and Fe(100) are 1.18 eV and 1.47 eV, respectively. The larger diffusion barrier into Fe(100) is mainly due to the stronger bonding between carbon and the Fe(100) surface. We predict that the rate-limiting step for C incorporation into bulk Fe is the initial diffusion to subsurface sites, while the rate-limiting step for absorbed carbon segregation to the surface is bulk diffusion, with no expected difference between rates to segregate to different surfaces. Lastly, we predict that graphite formation will be more favorable on C-covered Fe(110) than C-covered Fe(100).

DOI: 10.1103/PhysRevB.71.045402 PACS number(s): 68.43.Bc, 66.30.Jt, 68.47.De

I. INTRODUCTION

Iron as a cheap transition metal has been employed to catalyze reactions involving carbon-containing molecules. This often leads to individual carbon atoms interacting with Fe surfaces during the reactions. Desirable reactions include the formation of carbon nanotubes from gaseous hydrocarbons,[1–3] making gasoline from synthesis gas,[4] etc. On the other hand, coke formation on the catalyst surface[5] is undesirable as it poisons the catalyst. It is therefore of interest to study how isolated carbon atoms bind with Fe surfaces, as the first step towards understanding further reactions involving carbon interaction with other carbon atoms on the surface or with substrate Fe atoms to form carbide.

Another perspective of carbon-iron interactions is from materials science. When steels are subjected to carbonaceous gases such as CH_4 or CO, carburization[6] or metal dusting[7] can occur. In particular, CO dissociates readily on a steel surface and carbon atoms may diffuse into steels and form carbides. On the other hand, carbon atoms can segregate to Fe surfaces or grain boundaries when carbon-saturated steels are annealed. So the kinetics for carbon atoms diffusing in or out of Fe surfaces also plays a role in steel corrosion and steel-making processes.

Low-energy electron diffraction (LEED) indicates that adsorbed carbon atoms form a $c(2\times2)$ structure on Fe(100),[8,9] while a complex pattern of adsorbed carbon was observed on Fe(110).[10] Very few theoretical studies have examined the interaction between carbon atoms and Fe surfaces. Arabczyk and Rausche studied carbon atom adsorption on Fe(110) using extended Hückel theory (EHT) within a cluster model.[11] We will compare our results with theirs, demonstrating that EHT, essentially the tight-binding method, is not accurate enough to yield the correct site preference for carbon on Fe(110). Sorescu *et al.*[12] studied the interaction of carbon with Fe(100) when they were investigating CO adsorption on Fe(100) with gradient-corrected density-functional theory (DFT) and ultrasoft pseudopotentials. They found that C prefers the fourfold hollow site on Fe(100). They did not investigate the interaction of C with the Fe(100) subsurface.

In this work, we use spin-polarized DFT to study the interaction of carbon with two low-index single-crystal surfaces of body-centered-cubic Fe, namely Fe(110) and Fe(100). We examine the site preference of carbon on the surface, in the subsurface, and the diffusion of carbon into the surface. The rest of the paper is organized as follows. In Sec. II, we present the theoretical method employed. Results for carbon atom adsorption on Fe surfaces and absorption in Fe subsurfaces are presented in Secs. III A and III B, respectively. We then present the results for carbon diffusion into Fe surfaces in Sec. III C. We summarize and conclude in Sec. IV.

II. THEORETICAL METHOD

We perform first-principles calculations based on spin-polarized density-functional theory (DFT).[13,14] The Vienna Ab Initio Simulation Package (VASP) is used to solve the Kohn-Sham equations with periodic boundary conditions and a plane-wave basis set.[15–17] Here we employ Blöchl's all-electron projector augmented wave (PAW) method,[18] as implemented by Kresse and Joubert.[19] For the treatment of electron exchange and correlation, we use the generalized gradient approximation (GGA) of PBE.[20]

We use a kinetic energy cutoff of 400 eV for all the calculations; this converges the total energy of, e.g., ferromag-

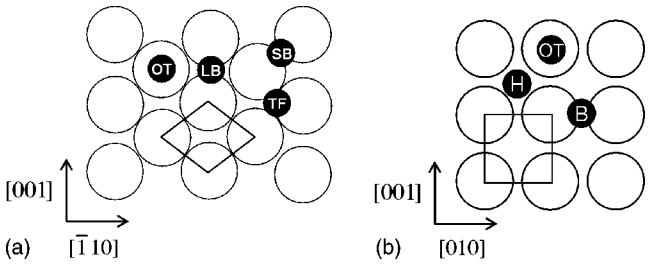

FIG. 1. High-symmetry adsorption sites on Fe surfaces. (a) Fe(110): OT denotes on top, SB denotes short bridge, LB denotes long bridge, and TF denotes threefold; (b) Fe(100): B denotes bridge, H denotes hollow. Surface (1×1) cells for both Fe(110) and Fe(100) are also shown.

netic (FM) bcc Fe to within 1 meV/at. The Monkhorst-Pack scheme[21] is used for the k-point sampling. An equilibrium lattice constant of 2.83 Å is used for ferromagnetic bcc Fe, as we obtained earlier with a converged k-mesh of $15\times15\times15$.[22] Fe(110) is the closest-packed surface of bcc Fe and is basically bulk-terminated, with little relaxation and no reconstruction.[23] Fe(100) is more open than Fe(110), but its interlayer relaxation is also small.[24] To model Fe(110) and Fe(100), we use slabs with seven layers, which we showed previously is sufficiently thick.[23] We put adsorbates on one side of the slab; this produces a dipole due to the charge rearrangement on the surface caused by adsorption, however we did not bother with a dipole correction to the total energy since it was very small (<0.01 eV/cell). Only the top three layers of the seven substrate layers are allowed to relax, together with the adsorbate layer. The bottom four layers are kept fixed in bulk positions to represent the semi-infinite bulk crystal beneath the surface. (Allowing the fourth layer of the substrate to relax only changes the total energy of the slab by ~5 meV.) When the maximum force acting on each relaxed atom of the slab drops below 0.01 eV/Å, the structural relaxation is stopped. We use converged[23] k-meshes of $14\times14\times1$, $7\times7\times1$, and $4\times4\times1$ for Fe(110) (1×1), (2×2), and (3×3) cells, respectively, and $12\times12\times1$, $6\times6\times1$, and $4\times4\times1$ for Fe(100) (1×1), (2×2), and (3×3) cells, respectively. A surface (1×1) cell is shown in Fig. 1 for both Fe(110) and Fe(100).

The adsorption energy of carbon atoms on Fe surfaces, and the absorption energy into Fe subsurface sites, are defined in the same manner, as given in Eq. (1),

$$\Delta E = E(\mathrm{Fe}_n\mathrm{C}) - E(\mathrm{Fe}_n) - E(\mathrm{C}). \quad (1)$$

Here all energies are referenced to an isolated carbon atom and a pure Fe slab. The first term on the right-hand side is the total energy of the slab that includes n Fe atoms and 1 C atom; the second term is the total energy of the slab that consists of n Fe atoms. The first two terms are calculated with the same parameters (k-point sampling, energy cutoff, etc.). The third term is the total energy of an isolated C atom in its ^{3}P ground state, which is estimated by putting a C atom in a cubic box with dimensions of 10 Å sides and carrying out a spin-polarized Γ-point calculation. We also want to compare the stability of the carbon adatom with that of graphite. Since the van der Waals interaction between graphite sheets is not described properly with DFT-GGA, we model graphite using the experimental geometry [$a=2.462$ Å and $c=6.656$ Å at 0 K (Ref. 25)] and do not optimize its structure. We calculate the total energy of graphite with a converged kinetic energy cutoff of 400 eV and a converged $8\times8\times4$ k-mesh.

The climbing image–nudged elastic band (CI-NEB) method[26] is used to locate the minimum energy paths (MEPs) and the transition states for C diffusion into Fe(110) and Fe(100). We use the (3×3) cell for studying diffusion into Fe(110) and Fe(100), which corresponds to 0.11 ML carbon coverage. We use a force tolerance of 0.02 eV/Å for the transition state search.

The natures of the relaxed adsorbate configurations and the saddle points found by the CI-NEB method are determined by diagonalizing a finite difference construction of the Hessian matrix with displacements of 0.02 Å (only allowing the C atom to move).

III. RESULTS AND DISCUSSION

A. Carbon adsorption on Fe(110) and Fe(100)

We first investigate how carbon atoms bind to Fe surfaces. Table I displays the adsorption energies of a carbon atom at 0.25 ML in high-symmetry sites of Fe(110) and Fe(100), as shown in Fig. 1. The adsorption data indicate that C atoms bind very strongly with Fe surfaces. At 0.25 ML, the C atom prefers the high coordination sites, namely the long-bridge (LB) site on Fe(110) and the hollow site on Fe(100). Those high coordination sites are also the only stable sites on their respective surfaces. The short-bridge (SB) site is the transition state for C diffusion on Fe(110) between neighboring LB sites, with a barrier of 0.96 eV at 0.25 ML. Likewise, the bridge site is a transition state for C atom diffusion on Fe(100) between neighboring hollow sites, with a barrier of 1.45 eV at 0.25 ML. The on-top (OT) site is a higher-order saddle point for both Fe(110) and Fe(100).

Our prediction of the site preference of carbon on Fe(100) agrees with experiment[8,9] and a previous DFT-GGA study[12]

TABLE I. Adsorption energies (ΔE, eV) of C atoms on Fe(110) and Fe(100) at $\Theta_C=0.25$ ML. The nature of the critical point is given in parentheses (min denotes minimum, ts denotes transition state, and hos denotes higher-order saddle point).

Surface	Fe(110)			Fe(100)		
site	LB	SB	OT	Hollow	Bridge	OT
ΔE	−7.77 (min)	−6.81 (ts)	−5.48 (hos)	−8.24 (min)	−6.79 (ts)	−5.22 (hos)

TABLE II. Adsorption energies (E_{ad}) of the C atom on the long-bridge site of Fe(110) and the hollow site of Fe(100) and the corresponding energies of formation (ΔH) of graphite and a pure Fe surface from carbon adsorbed on the Fe surface, at different carbon coverages. Here $\Delta H = E(\mathrm{Fe}_{surf}) + E(graphite) - E(\mathrm{C/Fe}_{surf})$, with Fe_{surf} being Fe(110) or Fe(100).

Θ_C (ML)		0.11	0.25	0.5	1.0
E_{ad} (eV)	Fe(110)	−7.92	−7.77	−7.06	−5.73
	Fe(100)	−8.33	−8.24	−8.28	−7.64
ΔH (eV)	Fe(110)	0.065	−0.085	−0.80	−2.12
	Fe(100)	0.49	0.39	0.44	−0.20

employing ultrasoft pseudopotentials. As mentioned in the Introduction, Arabczyk and Rausche[11] studied carbon on Fe(110) with extended Hückel theory using a cluster model. Their cluster contained 11 atoms, with only one or two atoms allowed to relax. They predicted that carbon prefers the threefold site on Fe(110), contrary to what we have found. We predict carbon prefers the long-bridge site, and we find that carbon relaxes to the LB site even if placed initially at the threefold site. Due to the finite and small size of their cluster, the minimal structural relaxation allowed, and the use of EHT, we believe their conclusion is incorrect.

Next we examine how the adsorption energy changes as the carbon atom coverage increases. Table II shows that the adsorption energy of C on Fe(110) becomes progressively less negative as Θ_C is increased from 0.11 ML to 1 ML, indicating a significant repulsion (~2.2 eV) between C atoms at high coverages. For Fe(100), the trend is quite different. The adsorption energy changes only slightly between 0.11 ML and 0.5 ML, and becomes less negative by 0.64 eV at 1 ML. LEED showed that an ordered $c(2\times2)$ structure of carbon on Fe(100) forms via equilibrium segregation of carbon-saturated iron.[8] That ordered structure corresponds to our 0.5 ML case. From Table II, we see that 0.5 ML is the optimally high coverage that carbon can achieve on Fe(100) without causing strong repulsion between carbon atoms, consistent with the equilibrium $c(2\times2)$ structure observed.

Formation of C-C covalent bonds on Fe surfaces can reduce the repulsion at higher coverages, consistent with the observation of graphite island formation.[27] To examine the adsorption data in another way, we compare energetics of the formation of graphite and a pure Fe surface to the energy for carbon adsorbed on the Fe surface. The results are also shown in Table II. One can see that the formation of graphite is energetically favorable on Fe(110) for $\Theta_C > 0.11$ ML and is strongly favorable at 0.5 ML and higher. Even at a low coverage of 0.11 ML, the stability of graphite plus a pure Fe(110) surface is about the same as adsorbed carbon on Fe(110). On Fe(100), the picture is quite different. Below 1 ML, adsorbed carbon atoms are preferred over graphite. At a high coverage of 1 ML, the graphite state is only 0.20 eV more stable than the adsorption state. Therefore, we predict a greater tendency to form graphite on Fe(110) than on Fe(100).

Comparing adsorption energies on Fe(100) and Fe(110), one can see that carbon binds more strongly to Fe(100). Even at a low coverage of 0.11 ML, the adsorption energy difference between the two surfaces is still ~0.40 eV. This can be explained by the closer distance between C and the subsurface Fe atom, as shown in Fig. 2. Due to the large interlayer spacing, C is coordinated only to four surface Fe atoms on Fe(110), while on Fe(100), C is coordinated to five Fe atoms, including one subsurface Fe atom. The distance between C and the subsurface Fe atom is 2.37 Å for Fe(110), but only 1.98 Å for Fe(100). A recent LEED study[9] shows that carbon is indeed fivefold-coordinated on Fe(100).

The aforementioned ordered $c(2\times2)$ structure of carbon on Fe(100) is most commonly observed by LEED. Detailed structural parameters (see Fig. 3) have been reported on this structure recently.[9] We compare in detail our theoretical predictions for the $c(2\times2)$ structure with experiment in Table III. The agreement is very good, indicating that PAW-GGA (PBE) correctly predicts the adsorption structure for c(2

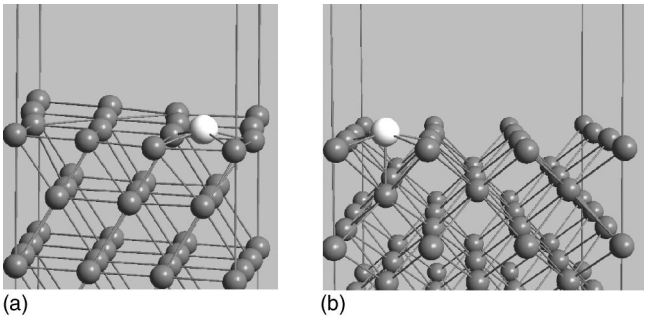

FIG. 2. Most stable structures of the C atom on Fe surfaces at 1/9 ML: (a) Fe(110); (b) Fe(100). Fe atoms are in gray and C in white.

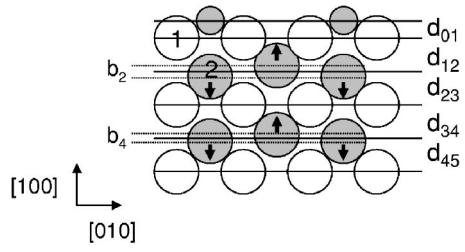

FIG. 3. Side view of the structural model for $c(2\times2)$-C on Fe(100). Small circles are C atoms and big circles are Fe atoms. Circles of the same color are in the same plane. d_{ij} is the interlayer spacing between layer i and layer j, with the zeroth layer being the adsorbate layer. b_i is the buckling magnitude in the ith substrate layer.

TABLE III. Comparison of the predicted [PAW-GGA (PBE)] structure of the structurally relaxed c(2 $\times$2) phase of carbon on Fe(100) with experiment. All parameters are in units of Å.

Parameters[a]	d_{01}	d_{12}	d_{23}	d_{34}	d_{45}	b_2	b_4	$L_{C\text{-}Fe1}$	$L_{C\text{-}Fe2}$
This work	0.30	1.52	1.40	1.44	1.43	0.13	0.02	2.03	1.89
Expt.	0.34	1.54	1.42	1.44	1.43	0.13	0.01	2.05	1.94

[a]See Fig. 3 for definitions of distances reported here. $L_{C\text{-}Fe1}$ and $L_{C\text{-}Fe2}$ denote the bond lengths from carbon to the first and second substrate Fe atoms, respectively.

$\times$2)-C on Fe(100), including the very short height of carbon above the first substrate layer, the adsorption-induced expansion between the first two substrate layers, the adsorption-induced buckling of the second substrate layer, and the short distance between carbon and the second-layer Fe atom.

B. Carbon absorption in the subsurfaces of Fe(110) and Fe(100)

In our earlier work,[22] we showed that the carbon atom prefers the high coordination octahedral (o) site in bulk Fe and the tetrahedral (t) site serves as the transition state for carbon diffusion between neighboring o-sites. We find that carbon atoms also prefer the o-sites in the subsurfaces, just as in the bulk. If we put the carbon atom initially at the subsurface t-site and let the system relax, carbon will move either to the surface or to the subsurface o-site.

Table IV displays the absorption energies of the carbon atom at the subsurface o-sites of Fe(110) and Fe(100) at 0.25 and 0.11 ML. Interestingly, carbon binds more strongly to the Fe(110) subsurface o-site than to the corresponding site on Fe(100), reversing the trend on the surface. As the Θ_C decreases from 0.25 ML to 0.11 ML, the absorption energy becomes more negative by 0.39 eV for Fe(100), narrowing the difference with Fe(110), for which the absorption energy does not change at these two coverages.

From our earlier work[22] on carbon dissolution and diffusion in bulk Fe, we know that carbon will cause a large tetragonal distortion to the host bcc lattice. We expect such a distortion also may occur when carbon atoms are present in the subsurface. Figure 4 shows the absorption structures at 0.11 ML. It is striking to see that one surface Fe atom coordinated to carbon is pushed toward vacuum by 0.5 Å for Fe(110), in order to reduce strain. The major distortion caused by carbon in Fe(100) is along a direction buried in the lattice, which can be seen by the significantly increased distances between two subsurface Fe atoms coordinated to carbon. This distortion is rather long range and propagates within the subsurface for several coordination shells. This also explains why the absorption energy becomes more negative by $\sim$0.40 eV for Fe(100) as the carbon atom coverage decreases from 0.25 ML to 0.11 ML (less distortion at lower coverage).

TABLE IV. The absorption energy (E_{ab}) in eV for the C atom in the subsurface of Fe(110) and Fe(100).

Θ_C (ML)	Fe(110)	Fe(100)
0.25	-7.30	-6.76
0.11	-7.30	-7.15

C. Carbon diffusion into Fe(110) and Fe(100)

Now that we have established the stable sites of the carbon atom on Fe surfaces and subsurfaces, we use the nudged elastic band method to obtain the minimum energy path (MEP) for carbon diffusion into the Fe surfaces. Figure 5 shows the converged MEP for carbon diffusion into Fe(110) at 0.11 ML. The energy change from the reactant to the product is 0.62 eV endothermic, indicating the carbon atom prefers to stay on the surface. We obtain a diffusion barrier of 1.18 eV going into the surface, while the reverse process has a barrier of 0.56 eV. At the transition state, the carbon atom resides in an approximate t-site comprising three Fe atoms on the surface and one Fe atom in the subsurface. Already at the transition state, one surface Fe atom is pushed up toward the vacuum somewhat. Going further into the surface, the carbon atom pushes the surface Fe atom even more toward the vacuum.

Figure 6 shows the converged MEP for carbon diffusion into Fe(100) at 0.11 ML. The energy change from the surface to the subsurface is 1.19 eV endothermic, 0.57 eV larger than that on Fe(110), indicating that the carbon atom prefers to stay on the surface even more for Fe(100). The diffusion barrier for carbon going into the surface is 1.47 eV. The MEP shows that the carbon atom first climbs uphill by $\sim$1.2 eV to reach a plateau, then moves uphill $\sim$0.3 eV to arrive at the transition state, and then goes downhill by $\sim$0.3 eV to the final state. At the transition state, carbon resides at a subsurface t-site, similar to carbon diffusion in bulk Fe.[22] Due to the small energy difference between the subsurface t-site and the subsurface o-site for Fe(100), the diffusion of the carbon atom from the subsurface to the surface is rather easy.

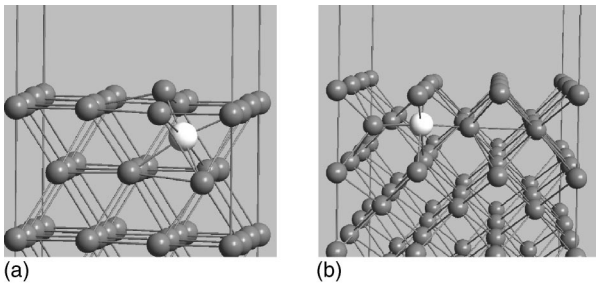

FIG. 4. Most stable structures of the C atom in Fe subsurfaces. (a) Fe(110); (b) Fe(100). Fe atoms are in gray and C in white.

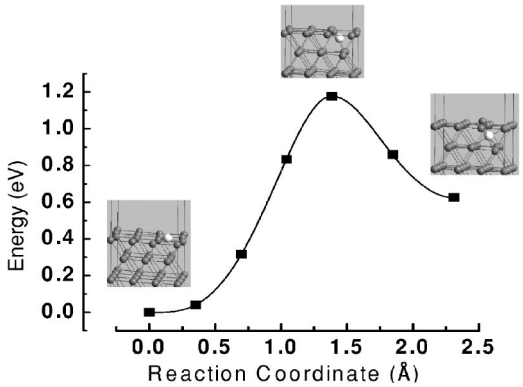

FIG. 5. Minimum energy path of C diffusion into Fe(110) and the structures for the initial, transition, and final states. Fe atoms are in gray and C in white.

Comparing the diffusion barriers for the carbon going into Fe surfaces, we see that it is easier for carbon to diffuse into Fe(110) than into Fe(100) by ~0.3 eV. This is mainly due to the stability of the initial state: because C binds more strongly (by ~0.4 eV) to Fe(100), it is more difficult for C to diffuse into Fe(100). If C then diffuses from subsurface sites further into bulk, we expect that C will encounter a barrier height similar to that for C diffusion in bulk Fe. This barrier height will be slightly higher (~0.10 eV) for Fe(110) than that for Fe(100) because C is more stable in the subsurface of Fe(110) (Table IV). In our earlier work,[22] we showed that the barrier for carbon diffusion through bulk Fe is 0.86 eV. So the barrier going from subsurface to bulk sites will be lower than that from surfaces to subsurfaces for both Fe(110) and Fe(100). In other words, the diffusion rates of adsorbed C atoms into surfaces will be determined by the first diffusion step (surface to subsurface).

Lastly, we consider the reverse process of segregation of dissolved C atoms to surfaces. Although the barrier of carbon diffusion from subsurfaces to surfaces is 0.26 eV higher for Fe(110) than that for Fe(100) [0.56 eV for Fe(110) and 0.30 eV for Fe(100)], they are both lower than the bulk value. Therefore, we expect the segregation rates of carbon atoms to Fe surfaces will be limited by bulk diffusion and similar rates will be observed segregating to either surface. This is indeed what experiments have shown.[28]

IV. SUMMARY AND CONCLUSIONS

Employing first-principles PAW-DFT-GGA techniques, we have studied carbon atom adsorption on, absorption in, and diffusion into Fe(110) and Fe(100). We find that the carbon atom binds strongly with Fe surfaces and prefers the long-bridge site on Fe(110) and the hollow site on Fe(100). The short-bridge site on Fe(110) and the bridge site on Fe(100) are transition states for carbon diffusion across the surfaces. The on-top sites on Fe(110) and Fe(100) are higher-order saddle points. The carbon atom binds more strongly with Fe(100) than with Fe(110) due to the fact that carbon is fivefold-coordinated on Fe(100).

The bonding between carbon and Fe(110) becomes less strong when the carbon coverage increases from 0.11 ML to 1 ML, due to lateral repulsions between carbon atoms. For Fe(100), we find a maximum coverage of 0.5 ML can be achieved without inducing strong repulsion among carbon atoms. This coverage corresponds to a $c(2\times2)$-C structure on Fe(100), which has been observed experimentally. Good agreement is achieved between our predictions and low-energy electron-diffraction data for this $c(2\times2)$-C structure. The tendency to form graphite is predicted to be much greater on Fe(110) than on Fe(100).

We find that carbon prefers the subsurface octahedral site in Fe(110) and Fe(100), as in the bulk Fe. The carbon atom is more stable in the subsurface o-site of Fe(110) versus Fe(100), since the distortion caused by the carbon atom is released by pushing one surface Fe atom towards vacuum by 0.5 Å in Fe(110), whereas in Fe(100) the strain remains in the lattice. As the carbon coverage decreases, the difference between the absorption energies in Fe(110) and Fe(100) lessens.

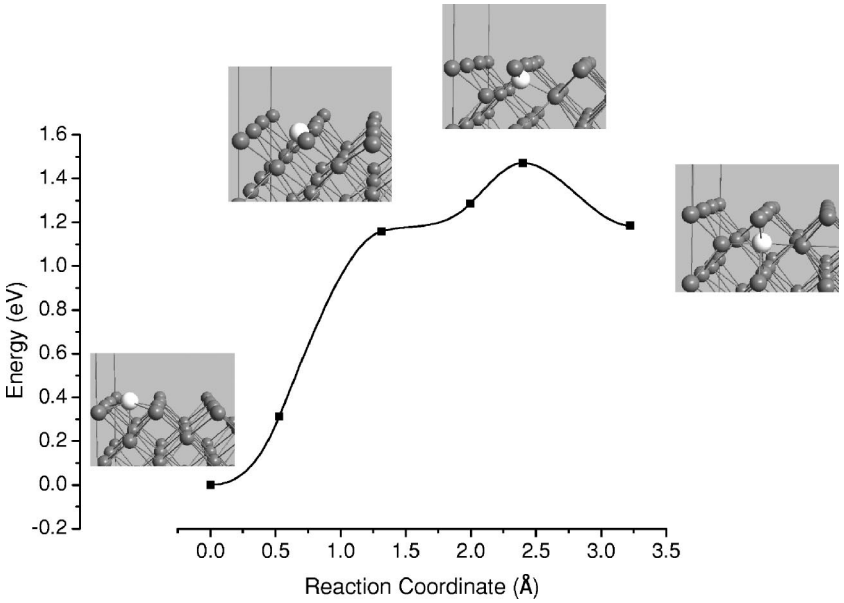

FIG. 6. Minimum energy path of C diffusion into Fe(100) and several structures along the path. Fe atoms are in gray and C in white.

Diffusion into Fe(110) is 0.62 eV endothermic with a barrier of 1.18 eV, while diffusion into Fe(100) is 1.19 eV endothermic with a barrier of 1.47 eV. In both diffusion processes, the transition state involves carbon in a subsurface tetrahedral site. The larger barrier into Fe(100) is mainly due to the stronger bonding between C and the Fe(100) surface.

Based on the above energetics and our earlier work on C diffusion and dissolution in bulk Fe, we find that C prefers to stay on the surface compared to residing in the subsurface and the bulk. This provides a driving force for dissolved C to segregate to the surface. We predict that the segregation rates will be determined by the bulk diffusion rate. At high temperature and high partial pressures of carbonaceous gases (such as CO or hydrocarbons) in the environment, adsorbed C can be driven into bulk Fe, and dissolution rates of adsorbed C atoms will be determined by the diffusion of C from surfaces to subsurfaces. Carburization is a complex process, involving C deposition on the surface, C diffusion into surfaces, and internal carbide formation. We have determined the barriers for the step of C diffusion between surfaces and subsurfaces. The kinetics of carburization will also need to include other factors, such as the kinetics of carbonaceous gas dissociation and the kinetics of carbide formation, which we will consider in future work.

ACKNOWLEDGMENTS

We are grateful to the Army Research Office for support of this work. We thank the Maui High Performance Computing Center and the NAVO Major Shared Resources Center for CPU time.

[1] H. Peng, T. Ristroph, G. Schurmann, G. King, J. Yoon, V. Narayanamurti, and J. Golovchenko, Appl. Phys. Lett. **83**, 4238 (2003).
[2] K. Nishimura, N. Okazaki, L. Pan, and Y. Nakayama, Jpn. J. Appl. Phys., Part 2 **43**, L471 (2004).
[3] A. Schaper, H. Hou, A. Greiner, and F. Phillipp, J. Catal. **222**, 250 (2004).
[4] R. Anderson, *The Fischer-Tropsch Synthesis* (Academic Press, Orlando, FL, 1984).
[5] G. Meima and P. Menon, Appl. Catal., A **212**, 239 (2001).
[6] H. Grabke, *Carburization: A High Temperature Corrosion Phenomenon* (Elsevier, Amsterdam, 1998).
[7] H. Grabke, Mater. High. Temp. **17**, 483 (2000).
[8] H. Grabke, W. Paulitschke, G. Tauber, and H. Viefhaus, Surf. Sci. **63**, 377 (1977).
[9] V. Blum, A. Schmidt, W. Meier, L. Hammer, and K. Heinz, J. Phys.: Condens. Matter **15**, 3517 (2003).
[10] S. Kelemen and A. Kaldor, J. Chem. Phys. **75**, 1530 (1981).
[11] W. Arabczyk and E. Rausche, Pol. J. Chem. **70**, 910 (1996).
[12] D. Sorescu, D. Thompson, M. Hurley, and C. Chabalowsk, Phys. Rev. B **66**, 035416 (2002).
[13] P. Hohenberg and W. Kohn, Phys. Rev. **136**, B864 (1964).
[14] W. Kohn and L. J. Sham, Phys. Rev. **140**, A1133 (1965).
[15] G. Kresse and J. Hafner, Phys. Rev. B **48**, 13 115 (1993).
[16] G. Kresse and J. Furthmüller, Phys. Rev. B **54**, 11 169 (1996).
[17] G. Kresse and J. Furthmüller, Comput. Mater. Sci. **6**, 15 (1996).
[18] P. E. Blöchl, Phys. Rev. B **50**, 17 953 (1994).
[19] G. Kresse and D. Joubert, Phys. Rev. B **59**, 1758 (1999).
[20] J. P. Perdew, K. Burke, and M. Ernzerhof, Phys. Rev. Lett. **77**, 3865 (1996).
[21] M. Methfessel and A. T. Paxton, Phys. Rev. B **40**, 3616 (1989).
[22] D. E. Jiang and E. A. Carter, Phys. Rev. B **67**, 214103 (2003).
[23] D. E. Jiang and E. A. Carter, Surf. Sci. **547**, 85 (2003).
[24] D. E. Jiang and E. A. Carter, Phys. Rev. B **70**, 064102 (2004).
[25] V. Ludsteck, Acta Crystallogr., Sect. A: Cryst. Phys., Diffr., Theor. Gen. Crystallogr. **A28**, 59 (1972).
[26] G. Henkelman, B. P. Uberuaga, and H. Jónsson, J. Chem. Phys. **113**, 9901 (2000).
[27] G. Panzner and W. Diekmann, Surf. Sci. **160**, 253 (1985).
[28] J. DuPlessis, P. Viljoen, and F. Bezuidenhout, Surf. Sci. **138**, 26 (1984).